Journal of Alloys and Compounds 509 (2011) 7922–7926

Contents lists available at ScienceDirect

Journal of Alloys and Compounds

journal homepage: www.elsevier.com/locate/jallcom

Thermoelectric properties of Sc- and Y-doped Mg_2Si prepared by field-activated and pressure-assisted reactive sintering

Q.S. Meng[a,*], W.H. Fan[a], R.X. Chen[a], Z.A. Munir[b]

[a] Department of Material Science and Engineering, Taiyuan University of Technology, Taiyuan 030024, China
[b] Department of Chemical Engineering and Materials Science, University of California, Davis, CA 95616, USA

ARTICLE INFO

Article history:
Received 18 August 2010
Received in revised form 7 May 2011
Accepted 10 May 2011
Available online 18 May 2011

Keywords:
Mg_2Si
Rare earth element doping
Thermoelectric material
FAPAS
Reactive sintering

ABSTRACT

Sc- and Y-doped-Mg_2Si samples were reactively sintered by the field-activated and pressure-assisted synthesis (FAPAS) method. The incorporation of these rare-earth elements in this silicide resulted in an n-type semiconductor. The addition of Sc and Y had no discernable effect on the lattice constant of Mg_2Si. The average grain size of the Y-doped Mg_2Si was about 2 μm, which was smaller than that of the sintered pure Mg_2Si. The power factor of samples doped with 2500 ppm Sc was consistently higher than that of pure Mg_2Si in the temperature range of 300–550 K. Similarly, the power factor of 2000 ppm Y doped Mg_2Si samples was higher than that of pure Mg_2Si over the temperature range of 300–675 K; the highest value being about 2.2×10^{-3} W m^{-1} k^{-2} at 468 K. This value is about two times that of the undoped Mg_2Si at the same temperature. The thermal conductivity of Mg_2Si doped with 2000 ppm Y was 80% of that of pure Mg_2Si. The highest figure of merit (ZT) for the Y doped (2000 ppm) samples was 0.23 at 600 K which was higher by a factor of 1.6 than the corresponding value of pure Mg_2Si at the same temperature. The results demonstrate the benefits of doping of Mg_2Si with Sc and Y in enhancing its thermoelectric properties.

1. Introduction

Magnesium silicide (Mg_2Si), a semiconducting intermetallic compound with a face-centered cubic CaF_2-type structure [1], has been identified as a promising n-type thermoelectric material in the temperature range of 500–800 K [2]. Compared with other materials with a figure of merit ZT > 1, Mg_2Si possesses many significant advantages, including the abundance of its constituent elements in nature, the non-toxicity of its processing by-products, and the benign nature of its environmental impact [3]. However, the thermal conductivity of Mg_2Si-based alloys is relatively high for thermoelectric applications, being about 6–8 W m^{-1} K^{-1} [4].

Attempts have been made to change both the electrical and thermal properties of this silicide through the addition of dopants and alloying elements, as well as thorough the modification of its microstructure [5–14]. Sakamoto et al. [6] investigated the use of Al as a partial substitute for Bi in Mg_2Si as a step to reduce the use of the toxic Bi. Liu et al. [7,14] investigated the influence of Sb doping on the thermoelectric properties of Sn-doped Mg_2Si using a two-step solid-state reaction and the ZT values was notably improved. A similar study was made by Luo et al. [8] to investigate the effect of Bi addition on the thermoelectric properties of Sn-doped Mg_2Si and showed that with an addition of 2.5 at.% Bi the material had a figure of merit of 0.78 at 800 K. The direct influence of Bi doping on the properties of Mg_2Si was investigated by Yang et al. [9], who reported a maximum figure of merit of 0.8 for 0.7 at.% Bi at 823 K. Gao et al. [10] used a B_2O_3 flux to synthesize Sn and Sb-doped Mg_2Si from the elements and reported a maximum power factor of 3.2×10^{-3} W m^{-1} K^{-2} at 610 K. Using induction melting and spark plasma sintering, Zhang et al. [11] synthesized Sn-doped dimagnesium silicide and investigated the effect of Sn doping on its thermoelectric properties. The highest figure of merit they obtained was 0.25 at 400 K.

The method of field-activated and pressure-assisted synthesis (FAPAS) has been successfully utilized in the preparation of thermoelectric materials. It was observed in our previous studies that products of β-$FeSi_2$ prepared by this method had a uniform, fine-grained structure and contained many micro-pores [15]. The pores contributed to a reduction in its thermal conductivity, and hence to the enhancement of its figure of merit. In the case of the formation of Mg_2Si by reactive sintering, the utilization of the FAPAS process is expected to contribute in two ways: (a) by shortening the time of the solid-state reaction between Mg and Si, and (b) by depressing the temperature of the solid-state reaction, thus suppressing the volatilization of Mg [16,17].

Efforts aimed at improving the thermoelectric properties of certain materials have recently been focused on the addition of rare

* Corresponding author. Tel.: +86 3516018254.
E-mail addresses: mengqingsen@263.net, mengqingsen1950@yahoo.com.cn (Q.S. Meng).

0925-8388/$ – see front matter © 2011 Elsevier B.V. All rights reserved.
doi:10.1016/j.jallcom.2011.05.033

Table 1
Compositions and designations of rare earth-doped Mg_2Si.

	Content of RE					
	Sc (ppm)			Y (ppm)		
	1000	2500	4000	1000	2000	3000
Sample designation	Sc-1	Sc-2	Sc-3	Y-1	Y-2	Y-3

earth (RE) elements [18–23]. This has been attributed to the role of the complex electronic shell and sharp energy-level splitting [24,25]. Studies involving the incorporation of Y and Sc [26–28] in thermoelectric materials have been carried out. It was shown that doping resulted in a decrease in the thermal conductivities [26]. The addition of Y_2O_3 to β-$FeSi_2$ resulted in the incorporation of Y on the Fe sub-lattice and the formation of a p-type material with a significantly higher Seebeck coefficient [27]. It was also reported that Y doping slightly accelerated densification during hot-pressing of $SrTiO_3$ [22,28]. In this paper we present results of an investigation on the effect of Sc and Y doping, as incorporated by the FAPAS method, on the thermoelectric properties of reactively sintered Mg_2Si.

2. Experimental

The starting materials used in this study were powders of Mg (99.95% pure, −80 −120 mesh), Si (99.95%, −200 mesh) and RE elements (Sc and Y: 99.99%, −200 mesh). All powders were obtained from Alfa Aesar-Johnson Matthey Co. (Ward Hill, MA). In the synthesis process, Sc and Y powders were added in different amounts aimed at producing Mg_2Si with different dopant levels. The level of addition of Sc and Y and the designation of the resulting samples are indicated in Table 1. Powders of Mg and Si were mixed to correspond to the stoichiometry of Mg_2Si along with the desired dopant level. The powder mixtures were then milled in a planetary mill (Fritsch, Model G5, Germany) at 230 rpm for 5 h. Zirconia balls (6 mm diameter) were used as the grinding medium. The ball-to-powder mass ratio used was 10:1. For comparison, we also prepared powders to form undoped Mg_2Si, similarly by reactive sintering. In this case powders of Mg and Si in the proper stoichiometric ratio were mixed and then milled in the planetary mill under the same conditions as above. Milling was aimed at homogenizing and activating the reactants; the latter contributes to enhancement of the sintering process. In all cases, 5 wt% excess Mg was added to compensate for the loss of Mg during milling and sintering [29].

The milled powders were placed in a cylindrical graphite die and cold-compacted into cylinders (20 mm in diameter and 2–3 mm in thickness) to a relative density in the range of 70–75%. These samples were then placed in the FAPAS apparatus (Fig. 1) and sintered at temperatures in the range of 1023–1073 K under a unixial pressure of 50 MPa for 15 min. Then the power was turned off and the samples were allowed to cool down naturally. The FAPAS method described here is similar to other methods: field activated sintering, including the spark plasma sintering (SPS) method and the field-assisted sintering technique (FAST).

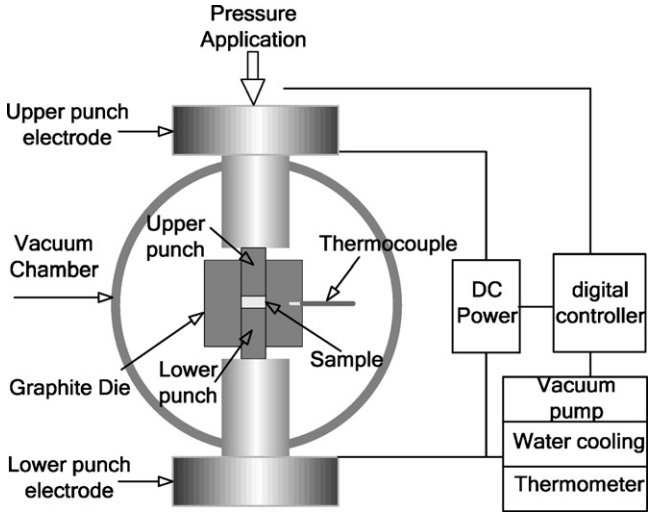

Fig. 1. Schematic diagram of the FAPAS apparatus.

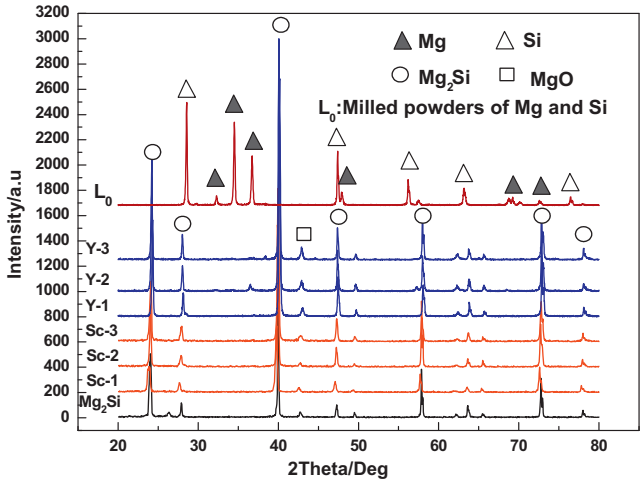

Fig. 2. XRD patterns of milled powders and sintered samples.

Phase and microstructural characterizations were made through X-ray diffraction, XRD (Model D5000, Siemens AG, Karlsruhe), scanning electron microscopy, SEM (Philips FEIXL30-SFEG), and optical microscopy, OM (OLYMPUS-GX71). Values of the Seebeck coefficient and the electrical conductivity were simultaneously determined by a Seebeck coefficient/electric resistance measurement system (ZEM-1, ULVAC Inc., Japan). A temperature difference of about 2–5 K between the cool and hot ends of the sample was used for the calculations of the Seebeck coefficient ($\alpha = V/\Delta T$). The thermal conductivity (κ) was calculated from $\kappa = \alpha D C_p$, where "a" is the thermal diffusivity (measured with a laser flash apparatus, Netsch, LFA457), D is the sample density (measured by a gravimetric method), and C_p is the specific heat capacity (measured on a thermal analyzer, Netsch, DSC404).

3. Results and discussion

3.1. Phases and microstructures

Fig. 2 shows the XRD patterns of the milled powders, the sintered Sc- and Y-doped samples, and the sintered undoped Mg_2Si sample. The patterns show that milling did not result in the formation of Mg_2Si, but that the complete formation of this silicide took place during the sintering process. The relative density of the sintered samples is in range of 95–97%, as determined by the Archimedes method. The lattice parameter of the resulting cubic Mg_2Si samples was evaluated from the XRD results, and the values showed no significant change with changes in the levels of the rare earth element additives used in this study.

Images of the microstructure of Mg_2Si are shown in Fig. 3. Doping with Y resulted in a reduction of grain size. The average grain sizes of undoped Mg_2Si (Fig. 3(a)) and the 2000 ppm Y-doped Mg_2Si (Fig. 3(b)) samples were in the ranges of about 3–4 μm and 1.5–2 μm, respectively.

3.2. Thermoelectric properties of doped Mg_2Si

3.2.1. Electric conductivity and Seebeck coefficient

The temperature dependence of the electric conductivity (σ) of Y- and Sc-doped Mg_2Si and pure (undoped) Mg_2Si is shown in Fig. 4(a). The conductivity of Sc-doped samples had a similar trend to that of undoped Mg_2Si, while the conductivity of samples doped with Y revealed a different behavior. The electric conductivity is defined by,

$$\sigma = nq\mu \quad (1)$$

where n is the carrier concentration, q is the carrier charge, and μ is the carrier mobility. Taking the sample Y-2 as an example, its conductivity increased from 2.61×10^4 to 3.74×10^4 S m^{-1} in the range of 288–378 K, which can be attributed to an increase

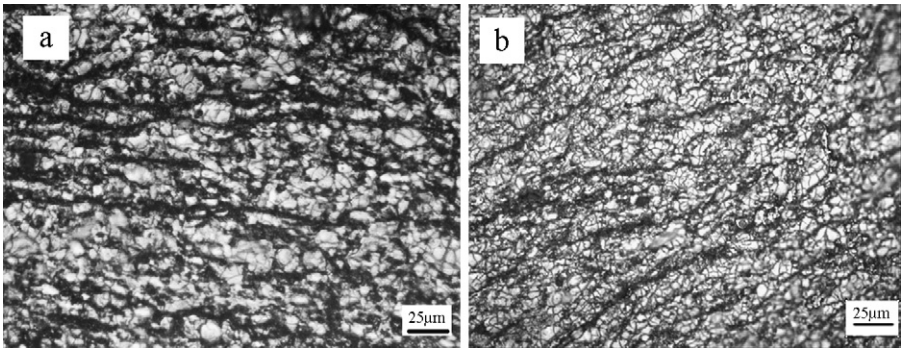

Fig. 3. Microstructure of fracture surfaces of undoped Mg_2Si (a) and Mg_2Si doped with 2000 ppm Y (b).

in carrier concentration arising from the introduction of Y. With a continued increase in temperature, lattice vibration leads to carrier scattering [30] and hence a decrease in conductivity, as can be seen by the value at 700 K, 0.98×10^4 S m^{-1}. At this and higher temperatures the increase in carrier concentration is balanced by an increase in lattice scattering and thus the conductivity remained relatively constant between 700 and 800 K [31].

The temperature dependence of the Seebeck coefficient, α, of Sc- and Y-doped Mg_2Si is shown in Fig. 4(b). The Seebeck coefficient of all samples was negative, and had a similar general trend with temperature. With one exception, the Seebeck coefficient of all samples investigated first increased to a maximum absolute value in the temperature range of about 600–700 K, and then decreased with further increase in temperature. The exception is sample Sc-2. This sample (Sc-doped at 2500 ppm) had the best Seebeck coefficient at a lower temperature (408 K). At this temperature the Seebeck coefficient is nearly two times that of the undoped Mg_2Si. The initial increase and subsequent decrease of α can be interpreted by the following relationship [32]:

$$|a_n| = \left| \frac{k_0}{q} \left[\frac{3}{2} + \ln \frac{2(2\pi m^* k_0 T)^{3/2}}{nh^3} \right] \right| \quad (2)$$

where α_n is Seebeck coefficient for an n-type thermoelectric material, k_0 is Boltzmann constant, h is Plank constant, n is the carrier concentration, and m^* is the carrier effective mass. For an optimal Seebeck coefficient, a high carrier effective mass and a low carrier density are required. In the temperature range of 300–580 K, the ionization of Sc (to contribute to conductivity) is not significant, however, doping by Sc increases the carrier effective mass, thus leading to a higher Seebeck coefficient. With an increase in temperature, a corresponding significant increase in carrier concentration is realized which leads to a decrease in the Seebeck coefficient. The Seebeck coefficient of the Y-doped Mg_2Si samples had a similar trend with temperature. With an increase in the dopant level, the observed higher Seebeck coefficient is attributed to an increase in lattice distortion.

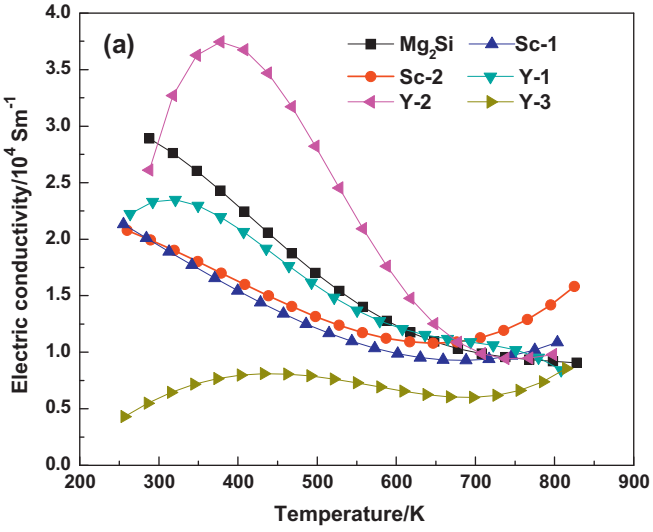

Fig. 4. Temperature dependence of (a) electric conductivity and (b) Seebeck coefficient for RE-doped Mg_2Si.

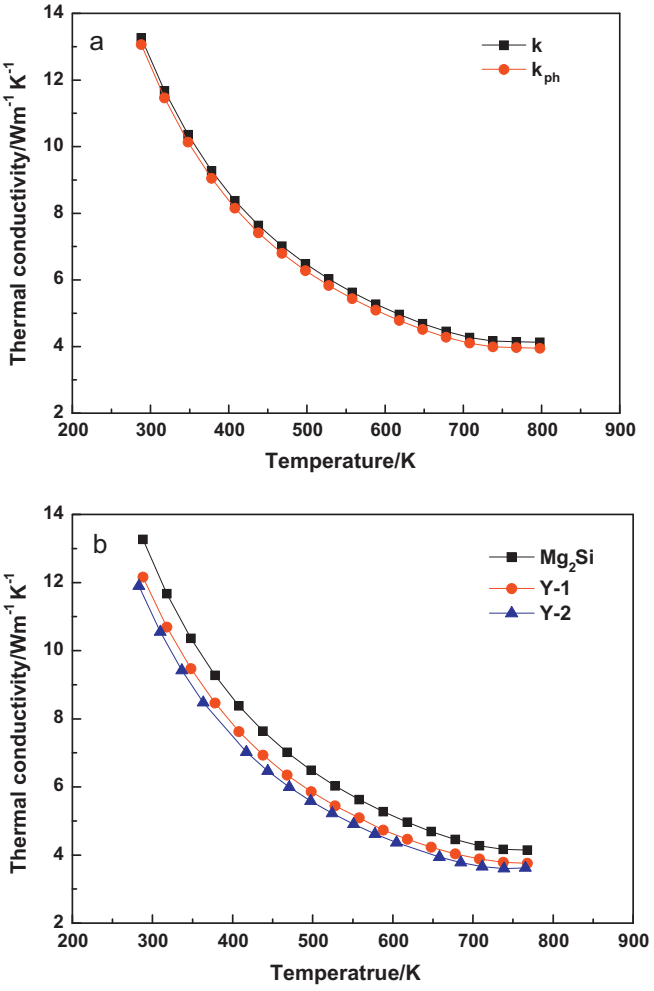

Fig. 5. Temperature dependence of (a) k and k_{ph} for pure Mg_2Si and (b) k for pure and Y-doped Mg_2Si.

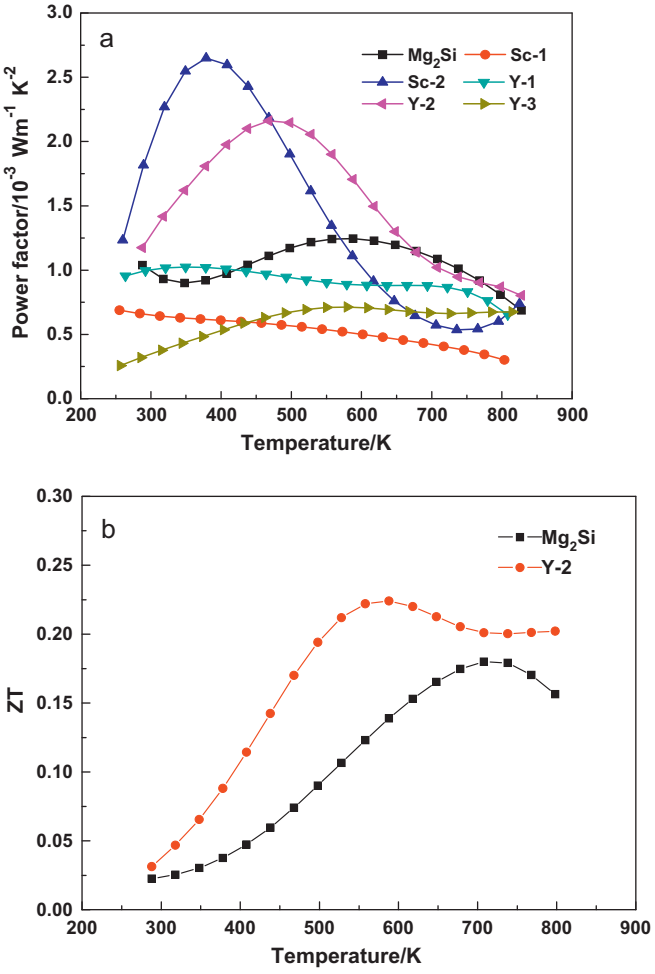

Fig. 6. Temperature dependence of (a) power factor (P) and (b) ZT for RE-doped Mg_2Si.

3.2.2. Thermal conductivity

The thermal conductivity of a material, k, is the sum of the electronic, k_{el}, and lattice (phononic), k_{ph}, conductivities, i.e., $k = k_{el} + k_{ph}$. The electronic conductivity, k_{el}, is calculated from the Wiedemann–Franz law [33] as:

$$k_{el} = L_0 \sigma T \quad (3)$$

where L_0 is the Lorentz number ($2.45 \times 10^{-8}\ V^2\ K^{-2}$), σ is the electrical conductivity, and T is the absolute temperature. Thus the contribution of lattice (phonons) to the thermal conductivity can be calculated by subtracting k_{el} from k. The temperature dependence of the thermal conductivity k and the lattice thermal conductivity k_{ph} for Mg_2Si is shown in Fig. 5(a). The present results are consistent with those reported by Tani and Kido [30,34]; the thermal conductivity of Mg_2Si was mainly influenced by k_{ph}, which is proportional to T^{-1}.

The thermal conductivity of samples doped with Y showed the same trend with temperature; they decreased monotonically in the measured temperature range, and decreased with more addition of Y due to lattice distortion, Fig. 5(b). The thermal conductivity of sample Y-2 is lower by 20% than that of undoped Mg_2Si.

3.2.3. Power factor and figure of merit

Fig. 6(a) shows the temperature dependence of the power factor, P, of Sc- and Y-doped Mg_2Si as well as that of undoped Mg_2Si. The power factor is defined by $P = \alpha^2\sigma$, where α is the Seebeck coefficient and σ is the electrical conductivity. The figure showed that

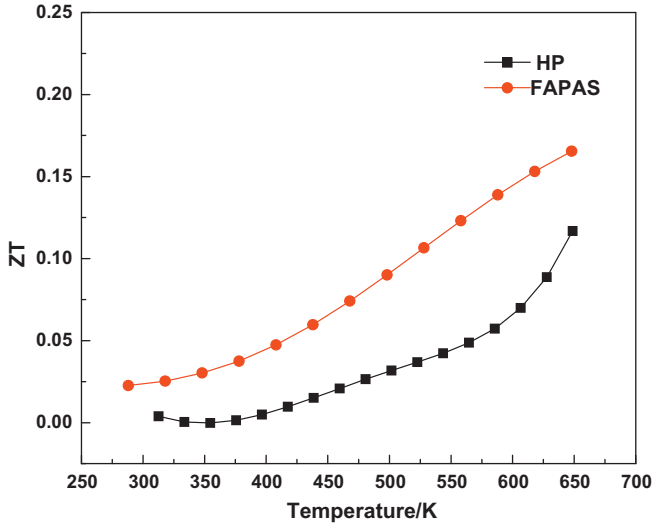

Fig. 7. Comparison of figure of merit, ZT, of Mg_2Si prepared by FAPAS (this work) and by HP.

doping with Sc and Y at the intermediate level (2500 ppm for Sc and 2000 ppm for Y) improved the power factor. For the 2500 ppm Sc-doped sample, P is higher by a factor of 1.3–2.9 than that of Mg_2Si in the temperature range of 250–550 K. This is due to the higher Seebeck coefficient in this temperature range (Fig. 4(b)). For the Y-doped sample, Y-2, P is higher over nearly the entire temperature range. For this sample, the highest value (at 468 K) is about 2 times the value of the undoped Mg_2Si at the same temperature. The maximum value of P (at 468 K) is $2.161 \times 10^{-3}\ W\ m^{-1}\ k^{-1}$.

The temperature dependence of the thermoelectric figure of merit, ZT (defined as $ZT = \alpha^2\sigma/k$), is shown in Fig. 6(b) for undoped and Y-doped Mg_2Si. Influenced by the thermal and electrical conductivity results, sample Y-2 has a significantly higher ZT than the undoped Mg_2Si, as shown in the figure. The maximum value of the figure of merit, ZT_{max}, for Y-2 is 0.23 at 600 K. At this temperature, the corresponding value for the undoped Mg_2Si is 0.14.

Thermoelectric Mg_2Si materials have also been prepared by a two-step process, which included a solid-state reaction of elemental powders and then a consolidation by hot-pressing (HP). Song et al. [35] prepared Sn-doped and undoped Mg_2Si from the elements through mechanical alloying followed by hot-pressing. A comparison between ZT values of the undoped samples prepared by these authors and corresponding values obtained in this study on undoped Mg_2Si prepared by the one-step reactive sintering is shown in Fig. 7. The ZT values obtained in this study are consistently higher than those of Song et al. [35] over the approximate temperature range of 300–650 K. In the range of 500–650 K, the ZT values obtained in this work are higher than those reported earlier by a factor ranging from roughly 1.5 to 3.0.

4. Conclusions

Yttrium and scandium-doped Mg_2Si (Sc: 1000–4000 ppm and Y: 1000–3000 ppm) was fabricated by the FAPAS process. Using milled elemental powder mixtures, reactive sintering resulted in dense (95–97%) silicide samples. SEM and optical microscopy images showed the samples to be microstructurally uniform. The addition of the rare earth elements resulted in smaller grains. The average grain size of Mg_2Si doped with 2000 ppm Y was in the range of 1.5–2.0 μm. The Seebeck coefficient of the Sc-and Y-doped Mg_2Si was higher than that of the pure silicide over the range of 300–600 K. The results showed that doping with Sc and Y (2500 ppm for Sc and 2000 ppm for Y) resulted in an improve-

ment in the power factor, *P*. For the 2500 ppm Sc-doped sample, *P* is higher by a factor of 1.3–2.9 than that of undoped Mg_2Si in the temperature range of 250–550 K. The maximum value of the figure of merit, ZT_{max}, for Y-doped Mg_2Si is 0.23 at 600 K. At this temperature, the corresponding value for the undoped Mg_2Si is 0.14.

Comparing the present results with those obtained on samples consolidated by hot-pressing showed a significant advantage. The ZT values obtained in this study are consistently higher than those consolidated by hot-pressing. In the range of 500–650 K, the ZT values obtained in this work are higher than those reported earlier by a factor ranging from roughly 1.5 to 3.0.

Acknowledgement

The studies were supported by the projects of the NSFC (No. 50975190).

References

[1] V.K. Zaitsev, M.I. Fedorov, E.A. Gurieva, I.S. Eremin, P.P. Kondtantinov, A.Yu. Samunin, M.V. Vedernikov, Phys. Rev. B 74 (2006) 045207.
[2] M. Akasaka, T. Iida, T. Nemoto, J. Soga, J. Sato, K. Makino, M. Fukano, T. Masataka, Y. Takanashi, J. Cryst. Growth 304 (2007) 196.
[3] W. Luo, M. Yang, F. Chen, Q. Shen, H. Jiang, L. Zhang, Mater. Sci. Eng. B 157 (2009) 96.
[4] V.K. Zaitsev, M.I. Fedorov, A.T. Burkov, E.A. Gurieva, I.S. Eremin, P.P. Konstantinov, A.Yu. Samunin, S. Sano, S.V. Ordin, M.V. Vedernikov, Proceedings of the 21st International Conference on Thermoelectrics, 2001, p. 151.
[5] H. Anno, K. Hatada, H. Shimizu, K. Matsubara, J. Appl. Phys. 83 (1998) 5270.
[6] T. Sakamoto, T. Iida, A. Matsumoto, Y. Honda, T. Nemoto, J. Sato, T. Nakajima, H. Taguchi, Y. Takanashi, J. Electron. Mater. 39 (2010) 1708.
[7] W. Liu, X. Tang, J. Sharp, Phys. D: Appl. Phys. 43 (2010) 085406.
[8] W.J. Luo, M.J. Yang, Q. Shen, H.Y. Jiang, L.M. Zhang, Adv. Mater. Res. 66 (2009) 33.
[9] M. Yang, W. Luo, Q. Shen, H. Jiang, L. Zhang, Adv. Mater. Res. 66 (2009) 17.
[10] H. Gao, T. Zhu, X. Liu, L. Chen, X. Zhao, J. Mater. Chem. 21 (2011) 5933.
[11] X. Zhang, Q.M. Lu, L. Wang, F.P. Zhang, J. Electron. Mater. 39 (2010) 1413.
[12] P. Zwolenski, J. Tobola, S. Kaprzyk, J. Electron. Mater. 40 (2011) 889.
[13] W.H. Fan, R.X. Chen, L.Q. Wang, P.D. Han, Q.S. Meng, J. Electron. Mater. 40 (2011) 1209.
[14] W. Liu, Q. Zhang, X.F. Tang, H. Li, J. Sharp, J. Electron. Mater. 40 (2011) 1062.
[15] Q.S. Meng, W.H. Fan, R.X. Chen, Z.A. Munir, J. Alloys Compd. 492 (2010) 303.
[16] J. Tani, H. Kido, Intermetallics 15 (2007) 1202.
[17] M. Umemoto, Y. Shirai, K. Tsuchiya, in: Proceedings of the Fourth Pacific Rim International Conference on Advanced Materials and Processing (PRICM4), Jpn. Inst. Met. (2001) 2145.
[18] S.Q. Bai, Y.Z. Pei, L.D. Chen, W.Q. Zhang, X.Y. Zhao, J. Yang, Acta Mater. 57 (2009) 3135.
[19] S. Bao, J. Yang, W. Zhu, X. Fan, X. Duan, J. Alloys Compd. 476 (2009) 802.
[20] H. Hashimoto, T. Kusunose, T. Sekino, J. Alloys Compd. 484 (2009) 246.
[21] S. Lemonnier, E. Guilmeau, C. Goupil, R. Funahashi, J.G. Noudem, Ceram. Int. 36 (2010) 887.
[22] M. Ito, T. Matsuda, J. Alloys Compd. 477 (2009) 473.
[23] Q. Zhang, J. He, X.B. Zhao, S.N. Zhang, T.J. Zhu, H. Yin, T.M. Tritt, J. Phys. D: Appl. Phys. 41 (2008) 185103.
[24] R.J. Gambino, W.D. Grobman, A.M. Toxen, J. Appl. Phys. Lett. 22 (1973) 506.
[25] G. Mahan, B. Sales, J. Sharp, Phys. Today 50 (1997) 42.
[26] H. Muta, K. Kurosaki, S. Yamanak, J. Alloys Compd. 350 (2003) 292.
[27] M. Ito, T. Tad, S. Katsuyam, J. Alloys Compd. 350 (2003) 296.
[28] A.V. Morozkin, V.N. Nikiforov, J. Alloys Compd. 400 (2005) 62.
[29] Q.S. Meng, L.Q. Wang, B.S. Li, L.Z. Ding, S.P. Chen, Adv. Mater. Res. 1639 (2009) 79–82.
[30] J. Tani, H. Kido, Physica B 364 (2005) 218.
[31] Q. Zhang, X.B. Zhao, T.J. Zhu, A.J. Zhou, Phys. Scripta T129 (2007) 123.
[32] G. Busch, U. Winkler, Helv. Phys. 20 (1954) 1067.
[33] N.W. Ashcroft and N.D. Mermin. Solid State Physics, Holt, Rinehart, Winston, New York, 1976.
[34] J. Tani, H. Kido, J. Alloys Compd. 466 (2008) 335–340.
[35] R.B. Song, T. Aizawa, J.Q. Sun, Mater. Sci. Eng. B 136 (2007) 111–117.